REVISTAMATÉRIA V.29 N.3
ISSN 1517-7076 articles e20240129, 2024

Optimization of tribological behavior of Aluminium (A356) composites using TGRA technique

Suvvari Chinni Krishna Venkata Ramana Murty Naidu[1], Suresh Vellingiri[2], Saravana Murthi Chinnasamy[3], Shanmugasundaram Brindavanam[4], Allwin Ebinesar Jacob Samuel Sehar[5], Srinivasnaik Mukuloth[6], Yuvaraj Kunnathur Periyasamy[7], Jitendra Mohan Giri[8], Javvadi Eswara Manikanta[9]

[1]Sri Venkateswara College of Engineering and Technology, Department of Mechanical Engineering. Srikakulam, Andhra Pradesh, India.

[2]KIT-Kalaignarkarunanidhi Institute of Technology, Department of Mechanical Engineering. Coimbatore, India.

[3]United Institute of Technology, Department of Robotics and Automation. Coimbatore, India.

[4]Adhiparasakthi College of Engineering, Department of Mechanical Engineering. Ranipet, India.

[5]Vel Tech Rangarajan Dr Sagunthala R&D Institute of Science and Technology, Department of Biotechnology. Chennai, India.

[6]School of Engineering Jawaharlal Nehru University, Department of Mechanical Engineering. New Delhi, India.

[7]Sri Krishna College of Engineering and Technology, Department of Mechanical Engineering. Coimbatore, India.

[8]Lloyd Institute of Engineering and Technology, Department of Mechanical Engineering. Greater Noida, India.

[9]Shri Vishnu Engineering College for Women, Department of Mechanical Engineering. Bhimavaram, Andhra Pradesh, India.

e-mail: scvrmn@gmail.com, winsureshv2011@gmail.com, murthi221080@gmail.com, bshanindia@gmail.com, drallwin@veltech.edu.in, srinivasmukuloth@gmail.com, cadyuva99@gmail.com, jmgiri@engineer.com, manijem66@gmail.com

ABSTRACT

Lightweight materials are the great demand in the aerospace sector to enhance system performance. The automotive, aerospace sector has utilized the composite materials to strengthen the physical and mechanical qualities of less weight materials and to improve their functionality. In this study, three different base matrix alloy combinations comprise the specimens being examined. Selective laser melting was used to combine boron carbide, graphite, and iron oxide powder (2.5, 5 and 7.5 wt.%) with an aluminium alloy matrix. Use the ASTM B-557M standards, specimens are prepared for testing the hybrid composite including such wear, and scanning electron microscopy. The purpose of the current study is to use Taguchi-based gray relational analysis (TGRA) to improve the wear parameters of aluminium matrix composite. Grey relationship study has shown that the optimal combinations for determining the hybrid composite's wear rate and coefficient of friction are 40 N load (level 3), 6 m/s sliding speed (level 3), and 1000 m sliding distance (level 1). Hybrid composites are said to have better wear properties and to offer enhanced components for the automotive, marine, and aerospace industries as compared to earlier metal matrix composites.

Keywords: Aluminium alloy; Selective laser melting; Wear; Grey Relational analysis.

1. INTRODUCTION

The aerospace industry has required new and advanced materials to increase the system efficiency and researchers are always turned the exploring new things to do for achieving the requirements of market demands [1]. Hybrid composite materials have been examined and identified that the aerospace sector has enhanced the quality while it is essentially unfeasible to create a certain improvement with a single matrix [2]. Aluminium and its alloy matrix are used more often than other matrix materials because to their low density, excellent machining, great fatigue strength, corrosion resistance, high strength, and increased wear resistance [3]. Aluminium alloy nano composites had been used recently to improve various physical, mechanical and chemical properties including better specific strength, high resistance to corrosion, thermal stability, higher hardness, relatively low elastic modulus, low density and resistance to creep and erosion [4, 5]. Aluminum casting alloys A356, which were derived from quickly castable aluminum served as the matrix material. These alloys were used to make aircraft parts that needed to be extremely strong. These parts also had to be lightweight and extremely durable,

Corresponding Author: Suresh Vellingiri Received on 25/03/2024 Accepted on 06/05/2024

DOI: https://doi.org/10.1590/1517-7076-RMAT-2024-0129

thus the A356 alloy was chosen because of its superior castability, weldability and corrosion resistance [6]. Boron carbide, which had a metallic appearance and black in color. It was the second strongest ceramic substance after diamond and cubic boron nitride. It was produced by heating carbon at a high temperature using an electric arc furnace [7]. However, by providing exceptionally high hardness, improved strength, chemical stability, and higher thermal stability, nano B_4C ceramic reinforcing particles have been used in recent years to improve the mechanical and wear properties of aluminium matrix composites [8]. Zeeshan Ali had produced two set of composite specimens designated as A356/40 µm B_4C and A356/90 µm B_4C and the assessment had found that the B_4C particle essence significantly improved the mechanical characteristics of the A356 composite such as ultimate tensile strength, breaking strength, and hardness [9]. There are conflicting findings in the literature about the impact of graphite on dry sliding wear, and it was employed in aluminium composites. The wear research process of film generation is not fully understood. For instance, according to some studies, graphite affects the mechanical and maybe even the tribological characteristics of composite materials [10]. The adequate graphite content has been claimed in some circumstances to provide the ideal characteristics [11]. Mahdavi and Akhlaghi had created the Al6061/Gr and Al6061/SiC/Gr composites applying in situ powder metallurgy techniques and outcomes of this production process significantly had affected the matrix's grain size, porosity, distribution of reinforcing particles and interfacial properties of the reinforcement matrix, which in turn affected the mechanical and tribological properties of such composites [12]. Despite Ferrous oxide (Fe_3O_4) being among the first permanent magnetic elements, it is still used today in high gradient magnetic separation, electrical goods, medical equipment, motors, and other advanced technologies [13]. Magnetic type iron oxide nanoparticles are used to fluctuate machinery, heavy transformers, diesel engines, converters, medical field etc., [14]. A probable ferrous oxide (Fe_3O_4) was thought to be a useful space filler because of its low cost and high free energy of aluminum interaction. The reaction had provided the additional energy for the process and improved the wettability of the magnetite and aluminum matrix making it a highly valued filler material [15]. Selective laser melting (SLM) was based on the layer-by-layer method, which was the possible method that could produce complicated components from powder [16]. It had many advantages include the ability to build complex components and close-to-net shapes while conserving time and resources [17]. It had become evident in recent years that meeting the demand for complex-shaped products in a range of industrial applications would be extremely difficult utilizing the traditional AMC fabrication techniques, such as stir casting, compo-casting, squeeze casting and welding [18]. The built AMCs had showed significantly improved processability, more refined microstructure, well-bonded functionality and optimized crystallographic texture compared to unstrengthen counterparts after undergoing the SLM process. These qualities had led to improvements in tensile strength, wear resistance and hardness [19]. Additionally, DU *et al*., had reported that the research in which two fabrication techniques—selective laser melting (SLM) and Friction Stir Processing. SLM and FSP were used to create Aluminium/Carbon Nano Tubes (CNTs) composites. When CNTs were dispersed through SLM rather than FSP, the SLM samples with CNTs had showed higher hardness, UTS, YS and elongation [20]. Taguchi's technique was utilized to minimize variance in production or experimental settings, therefore improving the quality and performance of items or processes. For finding the best settings, it had entailed the creating trials with a limited number of carefully selected elements and levels, then had used statistical techniques to analyze the results [21]. An approach for optimization and decision-making had utilized the term grey relational analysis, or GRA. It had come from the notion of gray systems and is especially helpful for systems that have ambiguous or insufficient information. GRA had considered the trend and data dispersion when had assessedhow comparable a reference series is to other series. It had assisted the discovering the most significant aspects and making decisions based on the correlations among variables [22]. Research on metal composites employing Grey Relational Analysis (GRA) and Taguchi's approach have been driven by compelling reasons such improved mechanical, thermal or electrical qualities over conventional metals. To obtain better and more desired qualities, systematically optimize variables have including the composition, processing parameters and heat treatment by using Taguchi's approach [23]. Both nano-SiC additives in EDM oil and the Taguchi-based COPRAS method were employed to improve performance metrics [24]. The pursuant to the assessment of the literature, till now there is no investigation carried out on tribological behavior of A356 reinforced with Gr-FE_3O_4-B_4C. It is a difficult but necessary task to determine the optimal parameters for the wear behavior of A356 reinforced with Gr-FE_3O_4-B_4C hybrid composites under varying loads, sliding speeds, and sliding distances. Using Taguchi's based gray relational analysis, the problem of A356 reinforced with Gr-FE_3O_4-B_4C hybrid composites may be addressed quite easily. Based on that, Taguchi's based gray relational analysis is used to determine the ideal parameters for the wear behavior of the A356 reinforced with Gr-FE_3O_4-B_4C hybrid composites under unreliable load, sliding speed and sliding distance.

2. MATERIALS AND METHODS

2.1. Materials

The experiment utilized A356 alloy powder as a matrix material (60 m, 2.662 g/cc), which was procured from Bhoomi Metal & Alloys located in Maharashtra. The reinforcement powders were acquired from Geepex Limited in Delhi, boron carbide powder (42 m, 2.18 g/cc), graphite powder (115 m, 2.31 g/cc), and iron oxide Powder (72 m, 5.2 g/cc) available in Jay Enterprises in Surat. A356-B4C-Gr-Fe3O4 hybrid composite powder samples (2, 4, and 6) were prepared in a planetary ball mill.

2.2. SLM method

SLM machinery (Make: Govt of India ARCI organization in Telangana, India) has utilized to manufacture the A356-B4C-Gr-FE3O4 specimens. An SLM machine is equipped with the fiber laser that has the wavelength of 1076 nm. A continuous laser with the range of (440–460) W power output and spot size of range (90–120) µm are also employed throughout the duration of the experiment. As previously mentioned in literature reviews, the SLM method is carried out under the vacuum condition to avoid the specimens from oxidizing and degrading. The chamber pressure is set at 0.87 psi. Furthermore, to analyze how the atmosphere influenced the make superiority, argon through the gas flow is added to the testing setting. Here to pressure specified above, the chamber is emptied. During laser irradiation, argon gas is used to provide flow for changing the chamber pressure to 1.5×10^3 Pa. The step-by-step SLM technique and process parameters are shown in Table 1 and Figure 1. To conduct the experiment, single-layer samples with a size of 14 mm by 30 mm are built using each combination of the process parameters [25].

2.3. Wear test experiment

The pin-on disc wear equipment of the ducom type, as shown in Figure 2, is used for the wear studies on the SLM machine-formed composites, and the wear test machine specifications are listed in Table 2. The wear test

Table 1: Process parameters of SLM.

PARAMETERS	VALUES
Fiber Laser	440–460 W
Spot sizes	90–120 µm
Scan processing speed	20 m/s
Build area	300 × 300 × 400 mm
Layer thickness	30–150 µm
Platform heating	300°C

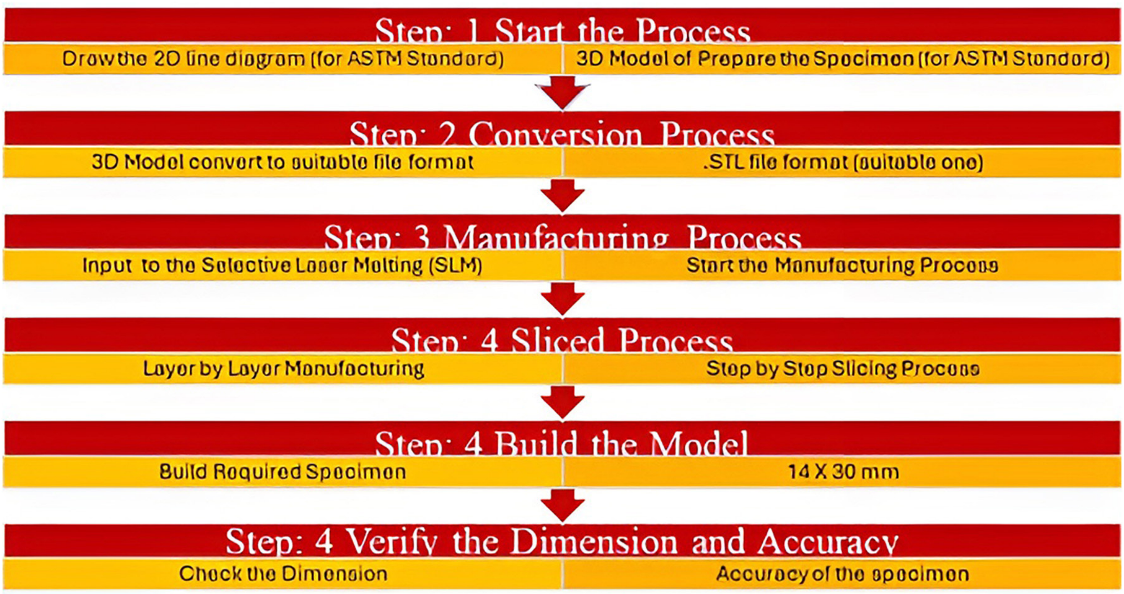

Figure 1: Step by step SLM technique.

Figure 2: Wear test experiment.

Table 2: Wear test machine specifications.

SPECIFICATIONS	VALUES
Disc size	165 mm × 8 mm
Normal Load	5 to 200 N
Rotational Speed	200 rpm to 2000 rpm
Frictional Force	up to 200 N
Wear measurement	range up to 2000 µm
Wear Track Diameter	140 mm
variable Pin/Ball Diameter	3, 6, & 10 mm

samples are prepared in according with ASTM B-557M standards and the dimensions of the sample pin are Ø12 mm and 25 mm in length. Samples are pressed in steel disc material of EN31with a surface roughness value of 0.1 and a hardness rating of RC 65. Before conducting the wear test, every samples are refined with different grade emery papers. The ends of the specimens are polished for metallography. An electronic scale with 0.0001 g minimum count is used to calculate the specimen's starting weight. The pin is pushed up against its counterpart and spun on the hardened EN31 steel plate at 65HRC. The samples are moved along the preset sliding path, cleaned with acetone, allowed to dry and then weighed to calculate the weight loss for wear.

2.4. Design of experiment and GRA

The Taguchi approach has involves doing the series of trials in an organized manner to eliminate variance in quality. For examine wear parameters and determine the combination of ideal characteristics that will lead to the decreased wear rate, the design of experiments technique [26] is utilized. In this approach, the experiment is carried out using a L27 orthogonal array and the procedure's key input parameters are load, sliding velocity and sliding distance. Table 3 depicts the levels of different input process parameters for the tests based on the L27 orthogonal array.

Table 3: Design of experiment and wear input parameters.

LEVEL	LOAD (N)	SLIDING VELOCITY (m/s)	SLIDING DISTANCE (m)
1	20	2	1500
2	30	4	2500
3	40	6	3500

The smaller the better attribute is employed to reduce wear. To identify statistically significant constraint, ANOVA is used. Based on the data gathered, signal-to-noise (S/N) ratios is determined. Because the S/N ratio is a standard metric, it shall be as high as possible. The S/N ratio may be calculated using Equation 1 with lower values preferred.

$$S/N \text{ ratio} = -10\ [\log \sum \left(B * B\right) / n] \tag{1}$$

Where,

B = responses for the given factor level combination and

n = number of responses

The grey system framework integrates Grey Relational Analysis (GRA) as an important component. A grey system encompasses both known and unknown information. Grey numbers are employed in this framework to represent interval-valued unknowns, offering a formal depiction of uncertainty that considers the accuracy of knowledge based on the width of the interval, in accordance with the theory of grey systems [27, 28].

2.5. Surface analysis

The presence of Gemini 500-M/s Carl Zeiss FESEM equipment is employed for analyzing specimen substrates under elevated magnifications (up to 200000×). For extracting the electrons, potential is applied. High temperature and extraction voltage work together has to improve the brightness and stability of the produced beam. The specimens are produced in accordance with ASTM E3-11 guidelines. The specimen measures 10 mm by Ø 10 mm.

3. RESULTS AND DISCUSSION

3.1. Wear test and GRA

Opening volume, final volume, volume loss, Wear loss and Coefficient of Friction (CoF) values are found the following equation.

$$\text{OVS} = \frac{OWS}{\rho} \tag{2}$$

Where,

OVS -Opening volume of the samples

OWS - Opening weight of the samples

ρ - Density of the samples

$$\text{CVS} = \frac{CWS}{\rho} \tag{3}$$

Where,

CVS - Closing volume of the samples

CWS - Closing weight of the samples

ρ - Density of the samples

$$\text{VLS} = \text{OVS} - \text{CVS} \tag{4}$$

Where,

VLS - Difference in samples volume loss

OVS - Opening volume of the samples

CVS - Closing volume of the samples

$$\text{WVS} = \frac{VLS}{SD} \tag{5}$$

Where,

WLS - Wear loss of the samples

VLS - Difference in samples volume loss

SD - Sliding distance

$$\text{CoF} = \frac{FF}{NF} \tag{6}$$

Where,

CoF - Coefficient of friction

FF - Frictional force

NF - Normal force

Equations 5 and 6 are used to get the wear loss and friction coefficient as illustrated in Table 4.

3.2. Optimization GRA

The Taguchi technique is the potent approach utilized in experimental and investigational works since it is required fewer tests to identify the response and perfect values of the wear parameters. It has done single-answer optimization tasks. As the result, the multi-objective method problem cannot be calculated using the traditional Taguchi methodology. Using grey relational analysis (GRA) and the Taguchi technique, multi-objective problems are computed. A decision-making and analysis tool is GRA.

Equation 7 contains the GRA technique's computing phases.

$$\text{yo} = (\text{yo}(1), \text{yo}(2), \text{yo}(3), \ldots \text{yo}(n)) \tag{7}$$

One of the often-used approaches for normalizing is linear data preparation. For wear loss, for instance, the "smaller is better" normalization option should be chosen. When normalizing wear loss data, values with low wear loss rates in linear normalization will take values close to "1," and values with high rates would take values close to "0." When smaller is preferable, normalization is carried out as in Equation 8.

$$\text{yi(s)} = \max(\text{yio(s)}) - \text{yio(s)}/\max(\text{yio(s)}) - \min(\text{yio(s)}) \tag{8}$$

Where

yi(s) - the gray relational structure rate, yo(s) - is the largest rate, max (yio(s)) and min (yio(s)) – are the largest and smallest rates of the yio(s) for the sth response.

3.2.1. Computation of grey relational coefficient analysis and grey relational grade analysis

In this stage, the grey relational coefficient is calculated to describe the relationship between the ideal and real experimental results. Equation 9 may be used to get the grey relationship coefficient.

$$\varepsilon_i(s) \frac{\Delta\min + \beth.\Delta\max}{\Delta oi(S) + \beth.\Delta\max} \tag{9}$$

Where, ε_i- grey relational coefficient, Δmin- is the smallest value of $\Delta oi(S)$, Δmax- is the largest value of $\Delta oi(S)$, $\Delta oi(S)$ - is the deviation sequence, $\beth$ - distinguished coefficient.

Table 4: The wear loss and friction coefficient.

EX. NO.	LOAD (N)	SLIDING VELOCITY (m/s)	SLIDING DISTANCE (m)	WEAR LOSS (mm^3/m)	FRICTION FORCE (N)	CoF
1	20	2	1500	0.00658	6.87	0.3435
2	20	2	1500	0.00785	6.91	0.3455
3	20	2	1500	0.00896	6.47	0.3235
4	30	2	2500	0.00943	9.84	0.328
5	30	2	2500	0.00643	9.12	0.304
6	30	2	2500	0.00549	9.47	0.315667
7	40	2	3500	0.00487	13.94	0.3485
8	40	2	3500	0.00397	13.63	0.34075
9	40	2	3500	0.00542	13.72	0.343
10	20	4	2500	0.00298	6.52	0.326
11	20	4	2500	0.00357	6.79	0.3395
12	20	4	2500	0.00491	6.27	0.3135
13	30	4	3500	0.00953	9.93	0.331
14	30	4	3500	0.00876	9.75	0.325
15	30	4	3500	0.00639	9.27	0.309
16	40	4	1500	0.00527	13.24	0.331
17	40	4	1500	0.00916	13.42	0.3355
18	40	4	1500	0.00837	13.64	0.341
19	20	6	3500	0.00743	6.13	0.3065
20	20	6	3500	0.00842	6.39	0.3195
21	20	6	3500	0.00586	6.82	0.341
22	30	6	1500	0.00739	9.61	0.320333
23	30	6	1500	0.00614	9.24	0.308
24	30	6	1500	0.00749	9.58	0.319333
25	40	6	2500	0.00864	13.18	0.3295
26	40	6	2500	0.00982	13.37	0.33425
27	40	6	2500	0.00834	13.52	0.338

$$\Delta oi(S) = |\mathrm{yo(s)} - \mathrm{yio(s)}|$$

$$\Delta\max = \max\max |\mathrm{yo(s)} - \mathrm{yjo(s)}| \quad (10)$$

$$\Delta\min = \min\min |\mathrm{yo(s)} - \mathrm{yjo(s)}|$$

Following the calculation of the grey relational coefficient, the grey relational grade for each performance feature is determined. Equation 10 may be used to get the grey relational grade.

$$\text{ɑ}\mathrm{i} = \frac{1}{n}\sum_{s=1}^{n} \varepsilon_i(s) \quad (11)$$

Where, ɑi–is the gray relational grade for the ith experiment and *n* – is the number of performance characteristics.

The experimental results are adjusted for normality using Equation 4 beginning with zero, and the standardized results are then translated into grey relational coefficients to reflect the connection among the expected and real information using Equation 5. Furthermore, the variation in the sequence is averaged to yield the grey relational grades, grey relational rank and their coefficient. Table 5 shows the wear rate, frictional force,

Table 5: Optimization and calculation of GRA.

WR (mm^3/m)	FF (N)	CoF	DEVIATION SEQUENCE			GREY RELATION COEFFICIENT			GRG	RANK
			WR (mm^3/m)	FF (N)	CoF	WR (mm^3/m)	FF (N)	CoF		
0.00658	6.87	0.724	0.00324	7.07	0.069	0.993562	0.06605	0.878735	0.646	16
0.00785	6.91	0.741	0.00197	7.03	0.052	0.996075	0.066401	0.905797	0.656	15
0.00896	6.47	0.762	0.00086	7.47	0.031	0.998283	0.062735	0.94162	0.668	13
0.00943	9.84	0.712	0.00039	4.1	0.081	0.999221	0.108696	0.860585	0.656	14
0.00643	9.12	0.685	0.00339	4.82	0.108	0.993266	0.093985	0.822368	0.637	19
0.00549	9.47	0.673	0.00433	4.47	0.12	0.991414	0.100604	0.806452	0.633	21
0.00487	13.94	0.616	0.00495	0	0.177	0.990197	1	0.738552	0.91	1
0.00397	13.63	0.586	0.00585	0.31	0.207	0.988435	0.617284	0.707214	0.771	8
0.00542	13.72	0.549	0.0044	0.22	0.244	0.991277	0.694444	0.672043	0.786	5
0.00298	6.52	0.597	0.00684	7.42	0.196	0.986505	0.063131	0.718391	0.589	26
0.00357	6.79	0.687	0.00625	7.15	0.106	0.987654	0.065359	0.825083	0.626	22
0.00491	6.27	0.729	0.00491	7.67	0.064	0.990275	0.0612	0.886525	0.646	17
0.00953	9.93	0.754	0.00029	4.01	0.039	0.99942	0.110865	0.927644	0.679	12
0.00876	9.75	0.784	0.00106	4.19	0.009	0.997884	0.10661	0.982318	0.696	11
0.00639	9.27	0.793	0.00343	4.67	0	0.993187	0.096712	1	0.697	10
0.00527	13.24	0.743	0.00455	0.7	0.05	0.990982	0.416667	0.909091	0.772	7
0.00916	13.42	0.692	0.00066	0.52	0.101	0.998682	0.490196	0.831947	0.774	6
0.00837	13.64	0.672	0.00145	0.3	0.121	0.997108	0.625	0.805153	0.809	3
0.00743	6.13	0.664	0.00239	7.81	0.129	0.995243	0.060168	0.794913	0.617	23
0.00842	6.39	0.541	0.0014	7.55	0.252	0.997208	0.062112	0.664894	0.575	27
0.00586	6.82	0.715	0.00396	7.12	0.078	0.992142	0.065617	0.865052	0.641	18
0.00739	9.61	0.673	0.00243	4.33	0.12	0.995164	0.10352	0.806452	0.635	20
0.00614	9.24	0.572	0.00368	4.7	0.221	0.992694	0.096154	0.693481	0.594	25
0.00749	9.58	0.623	0.00233	4.36	0.17	0.995362	0.102881	0.746269	0.615	24
0.00864	13.18	0.735	0.00118	0.76	0.058	0.997646	0.396825	0.896057	0.764	9
0.00982	13.37	0.751	0	0.57	0.042	1	0.46729	0.922509	0.797	4
0.00834	13.52	0.763	0.00148	0.42	0.03	0.997049	0.543478	0.943396	0.828	2

and coefficient of friction, as well as the deviation sequence, grey relational grade, grey relational rank, and coefficient.

Table 6 and Figure 3 have depicted the component effects depending on the value of the grey relationship grade. Although the grey relational grade assesses the degree of interaction among the sequence being evaluated and the comparative sequence, a higher number implies that the impartiality sequence is more closely connected to the reference sequence [29]. In simpler terms, a higher grey relational grade value equates to greater concert independent of the category of the performance characteristics [30]. As a result, the machining parameter level with the highest grey relational grade value is the best. The underlying sequence utilized in this case has the “Larger is better” characteristic. As a result, a comparison sequence with a higher grey relational grade will have a lower wear rate and coefficient of friction. The level with the highest average response is picked based on this notion. As demonstrated in Table 6 and Figure 3, the optimal factors for both the wear rate and the coefficient of friction attained for the hybrid composite are 40 N load (level 3), 6 m/s sliding velocity (level 3), and 1000 m sliding distance (level 1) combination.

3.3. Analysis of variance (ANOVA)

ANOVA is a statistical approach for analyzing experimental data. The effects of load, sliding velocity and sliding distance on wear are investigated using ANOVA in this study. This analysis is carried out with a level

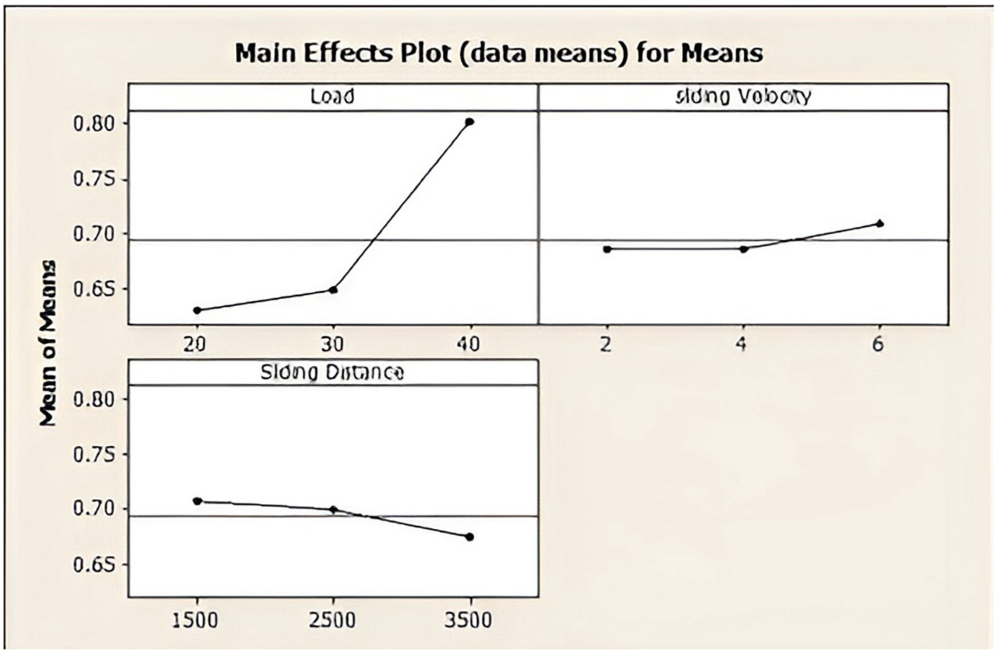

Figure 3: The component effects depending on the value of the grey relationship grade.

Table 6: Main effects on grey grades.

LEVEL	LOAD	SLIDING VELOCITY	SLIDING DISTANCE
1	0.632	0.698	0.714*
2	0.658	0.698	0.698
3	0.816*	0.724*	0.672
Delta	0.298	0.276	0.251
Rank	1	2	3

*Optimum values.

Table 7: Results of ANOVA on grey grade.

SOURCE	DF	ADJ. SS	ADJ.MS	F VALUE	P VALUE	%
Load	2	0.6453	0.6873	116.78	0.007	28.17
Sliding Velocity	2	0.7453	0.5789	186.29	0.005	45.16
Sliding Distance	2	0.5698	0.4756	108.26	0.008	26.32
Residual Error	2	0.0029	0.0035	–	–	0.35
Total	8	0.1456	–	–	–	100

of significance of 8% and a degree of confidence of 92%. Table 7 shows the ANOVA results for MMCs overall grey relationship grade. The table indicates that sliding velocity has a substantial impact. The influence of sliding velocity (45.16%) on the multi-performance characteristics of A356 with 6% B_4C-Gr-Fe_3O_4 composite is largest, subsequent to load (28.17%) and sliding distance (26.32%).

Similar research was conducted by IKUBANNI *et al*. [31]. They discovered that, according to Taguchi and Grey's relational analysis, the wear index and volume loss are most significantly influenced by speed when examining the tribological properties of an aluminum/silicon carbide (SiC)/palm kernel shell ash (PKSA) hybrid composite. DEY *et al*. [32], examined the wear and friction properties of Al2024/TiB_2 composite by employing Taguchi's L25 orthogonal array and Grey-fuzzy analysis techniques. The study focused on converting a multi-objective optimization issue into a single-objective optimization one. Through Analysis of Variance

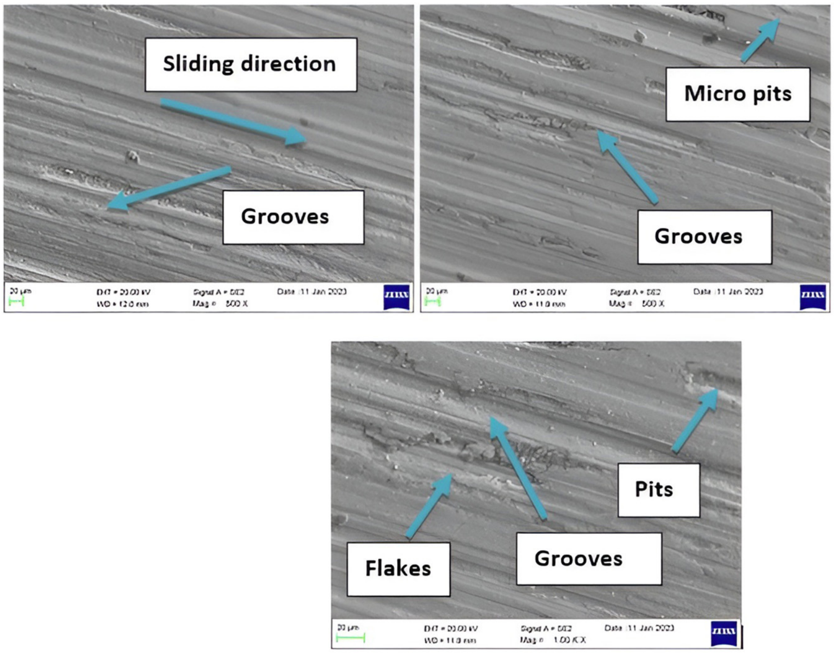

Figure 4: The fracture surface of samples A356 matrix with reinforcement 3, 6 and 9 wt% B_4C-Gr-Fe_3O_4.

(ANOVA) for grey fuzzy grade, it was determined that sliding distance stands out as the most influential parameter impacting the tribological behavior. SEM analysis of worn surfaces further illustrated that an escalation in sliding distance induces a shift in wear severity from mild to severe. SAM *et al*. [33] investigated a functionally graded A333/6wt.%B_4C/4wt.%ZrO_2 hybrid composite produced via horizontal-centrifuge casting, employing Taguchi's L27 orthogonal array. Their study focused on identifying the lowest specific wear rate and determining the optimum coefficient of friction (COF). UDAYA PRAKASH *et al*. [34] studied LM6/B_4C/Fly Ash hybrid composites using the cost-effective stir casting method. They employed the Design of Experiments (DoE) approach to conduct experiments and optimized them using Taguchi's Signal-to-Noise ratio (S/N) analysis. The study examined process parameters like Sliding Speed (S), Sliding Distance (D), Load (L), and Reinforcement Percentage (R%), focusing on Coefficient of Friction (COF) and Specific Wear Rate (SWR) as responses. The resulting composite, which combined aluminum alloy with B4C and Fly Ash, demonstrated advantages such as a reduced wear rate, lower density, and increased hardness compared to other composites and base alloys.

3.4. Surface morphology

Figure 4 depicts the etched fracture surface of samples A356 matrix with reinforcement 3, 6, and 9 wt.% B_4C-Gr-Fe_3O_4 and the distribution of reinforcements in different specimens, which is relevant for studying worn-out surface morphology. The Aluminium A356 alloy matrix has flows viscously in the form of a pin during sliding because it is softer than the material of the rubbing disc. This causes the specimen surface to flex plastically and results in significant material loss. As illustrated in Figure 4a, the worn surface of A356/3 wt.% B_4C-Gr-Fe_3O_4 composites has grooves, micro-pits and fractured oxide layer, which would have increased wear loss. Whereas reinforcement nanoparticles in A356 alloy-6wt% B_4C-Gr-Fe_3O_4, A356 alloy-9wt% B_4C-Gr-Fe_3O_4 composites restrict the viscous flow of the matrix, as shown in Figure 4b, c, the reduction in grooves or erosion with the addition of B_4C-Gr-Fe_3O_4 nanoparticles has increased resistance to wear loss. Meanwhile, stress has appeared to be transmitted on B_4C-Gr-Fe_3O_4 nanoparticles and strain concentration has occurred around these particles, with the addition of B_4C-Gr-Fe_3O_4 nanoparticles showing less and fewer fractures and grooves. Figures 4b, c show flakes, fewer and smaller grooves than Figure 4a indicating lower wear loss due to the individual action of hard B_4C-Gr-Fe_3O_4 nanoparticles. The viscous flow of the matrix is restricted by B_4C-Gr-Fe_3O_4 nanoparticles [35]. Meanwhile stress has appeared to be conveyed on B_4C-Gr-Fe_3O_4 nanoparticles with strain concentration occur in these nanoparticles. Because the reinforcing particles are soft, they function as solid lubricants and minimizing wear loss [36].

4. CONCLUSION

This work describes how to use Taguchi's orthogonal array in conjunction with grey relational analysis to optimize the wear rate, friction force, and coefficient of friction of A356/B4C-Gr-Fe_3O_4 hybrid metal matrix composites. Hybrid metal matrix composites, A356/B4C-Gr-Fe_3O_4, are effectively manufactured by Selective laser melting (SLM) techniques. The hybrid composite is found to have the best wear rate and coefficient of friction for the combination of 40 N load (level 3), 6 m/s sliding speed (level 3), and 1000 m sliding distance (level 1), as per the grey relational analysis. According to the ANOVA findings, sliding velocity (45.16%) has the highest influence on the multi performance properties of hybrid composite followed by load (28.17%) and sliding distance (26.32%). The study has discovered that an effective approach to optimize the multi-response properties of the manufactured composites, such as wear loss and coefficient of friction, is to combine Grey relational analysis with the Taguchi methodology. The confirmatory test carried out at a 93% confidence level revealed that the anticipated results are consistent with the actual experimental findings, falling within an acceptable range. Both methodologies utilized in this study exhibit reliability in the optimization of tribological properties. The newly developed hybrid composite has potential applications in engine blocks, pistons, rings, chassis components, and brake pads.

5. BIBLIOGRAPHY

[1] THANKACHAN, T., SOORYA PRAKASH, K., KAVIMANI, V., *et al.*, "Machine learning and statistical approach to predict and analyze wear rates in copper surface composites", *Metals and Materials International*, v. 27, n. 2, pp. 220–234, 2021. doi: http://doi.org/10.1007/s12540-020-00809-3.

[2] BHADRIRAJU, B., NARASINGAM, A., KWON, J.S.I., "Machine learning- based adaptive model identification of systems: application to a chemical process", *Chemical Engineering Research & Design*, v. 152, pp. 372–383, 2019. doi: http://doi.org/10.1016/j.cherd.2019.09.009.

[3] SURESH, V., SIVASUBRAMANIAN, R., MAGUTEESWARAN, R., "Investigation of aluminum and titanium based metal matrix composite", *International Review of Mechanical Engineering*, v. 6, n. 6, pp. 1175–1180, 2012.

[4] SAHARA, N., IKEDA, R., WU, S., *et al.*, "Effects of artificial aging on material properties of die-cast Al–Si–Cu–Mg–xNa alloy", *International Journal of Metalcasting*, v. 17, n. 1, pp. 515–525, 2023. doi: http://doi.org/10.1007/s40962-022-00793-x.

[5] SURESH, V., "An experimental and investigation on the micro-structure hardness and tensile properties of Al-GrFe_3O_4 hybrid metal matrix composites", *FME Transactions.*, v. 47, n. 3, pp. 511–517, 2019. doi: http://doi.org/10.5937/fmet1903511S.

[6] BANDIL, K., VASHISTH, H., KUMAR, S., *et al.*, "Microstructural, mechanical and corrosion behaviour of Al–Si alloy reinforced with SiC metal matrix composite", *Journal of Composite Materials*, v. 53, n. 28–30, pp. 4215–4223, 2019. doi: http://doi.org/10.1177/0021998319856679.

[7] KUMAR, S.D., RAVICHANDRAN, M., JEEVIKA, A., *et al.*, "Effect of ZrB_2 on microstructural, mechanical and corrosion behaviour of aluminium (AA7178) alloy matrix composite prepared by the stir casting route", *Ceramics International*, v. 47, n. 9, pp. 12951–12962, 2021. doi: http://doi.org/10.1016/j.ceramint.2021.01.158.

[8] XIA, H.M., ZHANG, L., ZHU, Y.C., *et al.*, "Mechanical properties of graphene nanoplatelets reinforced 7075 aluminum alloy composite fabricated by spark plasma sintering", *International Journal of Minerals Metallurgy and Materials*, v. 27, n. 9, pp. 1295–1300, 2020. doi: http://doi.org/10.1007/s12613-020-2009-0.

[9] SHARATH, B.N., VENKATESH, C.V., AFZAL, A., *et al.*, "Multi ceramic particles inclusion in the aluminium matrix and wear characterization through experimental and response surface-artificial neural networks", *Materials*, v. 14, n. 11, pp. 2895, 2021. doi: http://doi.org/10.3390/ma14112895. PubMed PMID: 34071305.

[10] AHMED, S.S., GIRISHA, H.N., KESHAVAMURTHY, R., "Impact of hot rolling on mechanical characteristics of AA7075/ TiB_2/graphite hybrid composites", *Journal of The Institution of Engineers (India): Series D*, v. 103, n. 1, pp. 191–201, 2022. doi: http://doi.org/10.1007/s40033-021-00311-z.

[11] BABU, T.V.B., SELVAM, M.A.J., NATRAYAN, L., "Improvising of dissimilar friction stir weld strengths using biosilica nanoparticle: mechanical, fatigue and microstructure properties", *Biomass Conversion and Biorefinery*, v. 14, n. 10, pp. 11435–11443, 2024. doi: http://doi.org/10.1007/s13399-022-03413-0.

[12] KARTHIGAIRAJAN, M., NAGARAJAN, P.K., RAVIRAJA MALARVANNAN, R., *et al*., "Effect of silane-treated rice husk derived biosilica on visco-elastic, thermal conductivity and hydrophobicity behavior of epoxy biocomposite coating for air-duct application", *Silicon*, v. 13, n. 12, pp. 4421–4430, 2021. doi: http://doi.org/10.1007/s12633-020-00772-z.

[13] SHAKERI, S., GHASSEMI, A., HASSANI, M., *et al*., "Investigation of material removal rate and surface roughness in wire electrical discharge machining process for cementation alloy steel using artificial neural network", *International Journal of Advanced Manufacturing Technology*, v. 82, n. 1–4, pp. 549–557, 2015. doi: http://doi.org/10.1007/s00170-015-7349-y.

[14] MONDAL, N., MANDAL, S., MANDAL, M.C., "FPA based optimization of drilling burr using regression analysis and ANN model", *Measurement*, v. 152, pp. 107327, 2020. doi: http://doi.org/10.1016/j.measurement.2019.107327.

[15] PALANIVEL, R., DINAHARAN, I., LAUBSCHER, R.F., "Application of an artificial neural network model to predict the ultimate tensile strength of friction welded titanium tubes", *Journal of the Brazilian Society of Mechanical Sciences and Engineering*, v. 41, n. 2, pp. 1–13, 2019. doi: http://doi.org/10.1007/s40430-019-1613-2.

[16] ZHANG, T., FENG, K., LI, Z., *et al*., "Effects of rare earth elements on the microstructure and wear properties of TiB^2 reinforced aluminum matrix composite coatings: experiments and first principles calculations", *Applied Surface Science*, v. 530, pp. 147051, 2020. doi: http://doi.org/10.1016/j.apsusc.2020.147051.

[17] RAVIKUMAR, M., REDDAPPA, H.N., SURESH, R., *et al*., "Optimization of wear behavior of Al7075/SiC/Al_2O_3 MMCs using statistical method", *Advances in Materials and Processing Technologies.*, v. 8, n. 4, pp. 4018–4035, 2022. doi: http://doi.org/10.1080/2374068X.2022.2036583.

[18] ELSHALAKANY, A.B., OSMAN, T.A., KHATTAB, A., *et al*., "Microstructure and mechanical properties of MWCNTs reinforced A356 aluminum alloys cast nanocomposites fabricated by using a combination of rheocasting and squeeze casting techniques", *Journal of Nanomaterials*, v. 2014, pp. 386370, 2014. doi: http://doi.org/10.1155/2014/386370.

[19] ABOULKHAIR, N.T., SIMONELLI, M., PARRY, L., *et al*., "3D printing of aluminium alloys: additive manufacturing of aluminium alloys using selective laser melting", *Progress in Materials Science*, v. 106, pp. 100578, 2019. doi: http://doi.org/10.1016/j.pmatsci.2019.100578.

[20] OLAKANMI, E.O., COCHRANE, R.F., DALGARNO, K.W., "A review on selective laser sintering/melting (SLS/SLM) properties, of aluminium alloy powders: processing, microstructure, and properties", *Progress in Materials Science*, v. 74, pp. 401–477, 2015. doi: http://doi.org/10.1016/j.pmatsci.2015.03.002.

[21] SAM, M., RADHIKA, N., RAMU, M., *et al*., "Optimizing reciprocal wear responses of centrifugally cast A333 hybrid functionally graded composite using Taguchi and response surface methodology", *International Journal on Interactive Design and Manufacturing*, v. 17, n. 3, pp. 1323–1338, 2023. doi: http://doi.org/10.1007/s12008-022-01125-3.

[22] BHARAT, N., BOSE, P.S.C., "Wear performance analysis and optimization of process parameters of novel AA7178/nTiO_2 using ANN-GRA method", *Proceedings of the Institution of Mechanical Engineers. Part E, Journal of Process Mechanical Engineering*, v. 238, n. 3, pp. 1409–1419, Jun. 2024. doi: http://doi.org/10.1177/09544089231156074.

[23] MISHRA, A., KUMAR, V., SRIVASTAVA, R.K., "Optimization of tribological performance of Al-6061T6-15% SiCp 15% Al_2O_3 hybrid metal matrix composites using Taguchi method & grey relational analysis", *Journal of Minerals & Materials Characterization & Engineering*, v. 2, n. 4, pp. 351–361, 2014. doi: http://doi.org/10.4236/jmmce.2014.24040.

[24] SELVARASU, S., SUBRAMANIAN, M., THANGASAMY, J., "An effect of nano-SiC with different dielectric mediums on AZ61/7.5% B4C nanocomposites studied through electrical discharge machining and Taguchi based complex proportional assessment method", *Matéria*, v. 28, n. 2, e20230058, 2023. doi: http://doi.org/10.1590/1517-7076-rmat-2023-0058.

[25] GAO, B., ZHAO, H., PENG, L., *et al*., "A review of research progress in Selective Laser Melting (SLM)", *Micromachines*, v. 14, n. 1, pp. 57, 2022. doi: http://doi.org/10.3390/mi14010057. PubMed PMID: 36677118.

[26] SREENIVASA IYENGAR, S.R., SETHURAMU, D., RAVIKUMAR, M., "Mechanical, wear, and fracture behavior of titanium diboride (TiB_2) - cerium oxide (CeO_2) reinforced Al-6061 hot-rolled hybrid composites", *Frattura ed Integrità Strutturale*, v. 17, n. 63, pp. 289–300, 2022. doi: http://doi.org/10.3221/IGF-ESIS.63.22.

[27] THANGAVEL, A., KUPPUSAMY, R., LAKSHMANAN, R., "Optimization of drilling parameters using GRA for polyamide 6 nanocomposites", *Matéria*, v. 28, n. 2, pp. 1–10, 2023. doi: http://doi.org/10.1590/1517-7076-rmat-2022-0337.

[28] ANTIL, P., ANTIL, S.K., PRAKASH, C., *et al*., "Multi-objective optimization of drilling parameters for orthopaedic implants", *Measurement and Control*, v. 53, n. 9–10, pp. 1902–1910, 2020. doi: http://doi.org/10.1177/0020294020947126.

[29] ZHANG, S., YAN, H., ZHANG, L., *et al*., "Effect of graphene nanosheets on microstructure and corrosion resistance of ADC12 alloy", *Journal of Materials Engineering and Performance*, v. 32, pp. 3590–3601, 2023. doi: http://doi.org/10.1007/s11665-022-07363-6.

[30] DEY, D., BHOWMIK, A., BISWAS, A., "Characterization of physical and mechanical properties of aluminium based composites reinforced with titanium diboride particulates", *Journal of Composite Materials*, v. 55, n. 14, pp. 1979–1991, 2021. doi: http://doi.org/10.1177/0021998320980800.

[31] IKUBANNI, P.P., OKI, M., ADELEKE, A.A., *et al*., "Optimization of the tribological properties of hybrid reinforced aluminium matrix composites using Taguchi and Grey's relational analysis", *Scientific American*, v. 12, e00839, 2021. doi: http://doi.org/10.1016/j.sciaf.2021.e00839.

[32] DEY, D., BHOWMIK, A., BISWAS, A., "A grey-fuzzy based multi-response optimisation study on the friction and wear characteristics of titanium diboride reinforced aluminium matrix composite", *Proceedings of the Institution of Mechanical Engineers. Part B, Journal of Engineering Manufacture*, v. 237, n. 14, pp. 2227–2239, 2023. doi: http://doi.org/10.1177/09544054221147973.

[33] SAM, M., RADHIKA, N., RAMU, M., *et al*., "Optimizing reciprocal wear responses of centrifugally cast A333 hybrid functionally graded composite using Taguchi and response surface methodology", *International Journal on Interactive Design and Manufacturing*, v. 17, n. 3, pp. 1323–1338, 2023. doi: http://doi.org/10.1007/s12008-022-01125-3.

[34] UDAYA PRAKASH, J., ANANTH, S., JEBAROSE JULIYANA, S., *et al*., "Parametric optimization of wear parameters of hybrid composites (LM6/B_4C/fly ash) using Taguchi technique", *Frontiers of Mechanical Engineering*, v. 9, pp. 1279481, 2023. doi: http://doi.org/10.3389/fmech.2023.1279481.

[35] XIONG, J., YAN, H., ZHONG, S., *et al*., "Effects of Yb addition on the microstructure and mechanical properties of As-cast ADC12 alloy", *Metals*, v. 9, n. 1, pp. 108, 2019. doi: http://doi.org/10.3390/met9010108.

[36] MURUGADOSS, P., JEYASEELAN, C., "Utilization of silicon from lemongrass ash reinforcement with ADC 12 (Al-Si alloy) aluminium on mechanical and tribological properties", *Silicon*, v. 15, n. 3, pp. 1413–1428, 2023. doi: http://doi.org/10.1007/s12633-022-02119-2.